

Coiled Coil Peptides as Universal Linkers for the Attachment of Recombinant Proteins to Polymer Therapeutics

Michal Pechar,^{*,†} Robert Pola,[†] Richard Laga,[†] Karel Ulbrich,[†] Lucie Bednárová,[‡] Petr Maloň,[‡] Irena Siegllová,[§] Vlastimil Král,[§] Milan Fábry,[§] and Ondřej Vaněk^{||}

[†]Institute of Macromolecular Chemistry, Academy of Sciences of the Czech Republic, Heyrovského nam. 2, 162 06, Prague 6, Czech Republic

[‡]Institute of Organic Chemistry and Biochemistry, Academy of Sciences of the Czech Republic, Flemingovo nam. 2, 166 10 Prague 6, Czech Republic

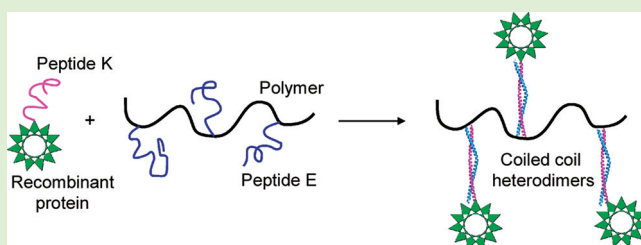
[§]Institute of Molecular Genetics, Academy of Sciences of the Czech Republic, Flemingovo nam. 2, 166 10 Prague 6, Czech Republic

^{||}Department of Biochemistry, Faculty of Science, Charles University in Prague, Hlavova 8, 128 40 Prague, Czech Republic

Supporting Information

ABSTRACT: We have designed, synthesized, and characterized peptides containing four repeats of the sequences VAALEKE (peptide E) or VAALKEK (peptide K). While the peptides alone adopt in aqueous solutions a random coil conformation, their equimolar mixture forms heterodimeric coiled coils as confirmed by CD spectroscopy. 5-Azidopentanoic acid was connected to the N-terminus of peptide E via a short poly(ethylene glycol) spacer. The terminal azide group enabled conjugation of the peptide with a synthetic drug carrier based on the *N*-(2-hydroxypropyl)methacrylamide copolymer containing propargyl groups using “click” chemistry.

When incorporated into the polymer drug carrier, peptide E formed a stable noncovalent complex with peptide K belonging to a recombinant single-chain fragment (scFv) of the M75 antibody. The complex thereby mediates a noncovalent linkage between the polymer drug carrier and the protein. The recombinant scFv antibody fragment was selected as a targeting ligand against carbonic anhydrase IX—a marker overexpressed by tumor cells of various human carcinomas. The antigen binding affinity of the polymer–scFv complex was confirmed by ELISA. This approach offers a well-defined, specific, and nondestructive universal method for the preparation of protein (antibody)-targeted polymer drug and gene carriers designed for cell-specific delivery.



INTRODUCTION

Hybrid copolymers consisting of both synthetic and natural macromolecules have become attractive materials for various biomedical applications.¹ Conjugation of biologically active proteins (e.g., antibodies, enzymes, and antibody fragments) to synthetic hydrophilic polymer carriers often improves the pharmacokinetics of the proteins, prolongs their blood circulation, reduces unwanted immunogenicity, slows down proteolytic degradation, and increases the accumulation of macromolecular therapeutics in solid tumors by an enhanced permeation and retention (EPR) effect.²

Antibodies and their fragments have been described as very efficient ligands for the specific targeting of both solid tumors and leukemia cells.^{3–5} However, covalent attachment of the two macromolecules (protein and synthetic polymer) is often nonselective (multiple functional groups of the protein are modified); the resulting polymer–protein conjugate is a complex mixture of macromolecules with high polydispersity and compromised biological activity. The precisely defined structure of the conjugate is highly desirable to achieve the optimal biological activity of the product. Last but not least, well-defined chemical entities obtain regulatory approval for

clinical applications more easily. The specific supramolecular noncovalent self-assembly of the two macromolecules represents a feasible solution for the general problem.

A heterodimeric coiled coil interaction has been recently reported^{6–9} as a linkage between biologically active molecules and synthetic hydrophilic polymers. In this work, we suggest using a coiled coil motif as a universal tool to bind recombinant proteins to synthetic hydrophilic polymers. We report here on the unique combination of recombinant technology and polymer chemistry for the preparation of a new class of well-defined targeted polymer therapeutics. It has been shown that attachment of a synthetic polymer to the coiled coil peptide does not disturb the coiled coil domain formation. On the contrary, the thermal stability of the polymer-modified coiled coil was even increased.^{10,11}

We have designed and synthesized the peptides (VAALEKE)₄ (peptide E) and (VAALKEK)₄ (peptide K), forming coiled coil heterodimers in aqueous solution. Peptide K was

Received: June 30, 2011

Revised: August 19, 2011

Published: August 25, 2011

incorporated into the structure of a recombinant single-chain fragment (scFv) of the M75 antibody without changing the structure of the binding part of scFv.

The antibody is known^{12–14} to specifically bind to carbonic anhydrase IX (CA IX), which is a transmembrane protein overexpressed in a wide variety of tumor cell types. Peptide E was covalently bound to a synthetic hydrophilic copolymer based on *N*-(2-hydroxypropyl)methacrylamide (HPMA) using “click” chemistry. A stable noncovalent complex was formed upon mixing the recombinant protein with the polymer under physiological conditions due to the formation of intermolecular coiled coil heterodimers. We have investigated receptor-specific cell binding (to CA IX) of the polymer–protein complex using ELISAs.

The combination of synthetic polymer and peptide chemistry with recombinant DNA technology described in this paper offers a new approach for the preparation of polymer–protein conjugates for cell-specific therapy. The specific noncovalent and nondestructive attachment of a recombinant protein (e.g., targeting antibody fragment) to a synthetic hydrophilic polymer via the coiled coil interaction is the major advantage of the presented method. The polymer–protein conjugates prepared by the self-assembly method can be used as targeted polymer antitumor therapeutics or diagnostics.

EXPERIMENTAL SECTION

Materials and Methods. 1-Aminopropan-2-ol, 2,2'-azobis(isobutyronitrile) (AIBN), *N,N*-dimethylformamide (DMF), dimethyl sulfoxide (DMSO), ethane-1,2-dithiol (EDT), 1,1,1,3,3,3-hexafluoroisopropan-2-ol (HFIP), glycylglycine, ethyldiisopropylamine (DIPEA), 1-hydroxybenzotriazole (HOBt), methacryloyl chloride, phenol, piperidine, thioanisole, trifluoroacetic acid (TFA), triisopropylsilane (TIPS), and all other reagents and solvents were purchased from Sigma-Aldrich (Czech Republic). 2-Chlorotriethyl chloride resin, TentaGel Rink amide resin, (benzotriazol-1-yloxy)-trispyrrolidinophosphonium hexafluorophosphate (PyBOP), 9-fluorenylmethoxycarbonyl (Fmoc), *tert*-butoxycarbonyl (Boc), *tert*-butyl (tBu) amino acid derivatives, and α -*O*-(2-carboxyethyl)- ω -*O*-(2-Fmoc-aminoethyl)tetraethylene glycol (Fmoc-Peg₄) were purchased from Iris Biotech, GmbH, Germany. 2-Hydroxy-4-methoxybenzyl (Hmb) and pseudoproline ($\psi^{Me,Me}$ pro) amino acid derivatives were from Merck. α -*O*-(2-Carboxyethyl)- ω -*O*-(2-Fmoc-aminoethyl) heptacosethylene glycol (Fmoc-Peg₂₇) was purchased from Polypure AS, Norway. All amino acids were of L-configuration. Methacryloyl chloride, 1-aminopropan-2-ol, and dichloromethane were distilled immediately before use. All chemicals and solvents were of analytical grade. Solvents were purified and dried using standard procedures. Monitoring of the conjugation of the peptide to the reactive copolymer was performed by HPLC using column Chromolith Performance RP-18e, 100 × 4.6 mm (Merck, Germany), and a linear gradient of water–acetonitrile, 0–100% acetonitrile in the presence of 0.1% TFA with a UV–vis diode array detector (Shimadzu, Japan). Determination of the molecular weights and polydispersities of the copolymers was carried out by size exclusion chromatography (SEC) on a HPLC system (Shimadzu) equipped with refractive index, UV, and multiangle light scattering DAWN 8 EOS (Wyatt Technology Corp., Santa Barbara, CA) detectors using a Superose 6 PC 3.2/30 or Superose 12 PC 3.2/30 column (Pharmacia) and 0.05 M phosphate buffer with 0.15 M NaCl, pH 6.5, at a flow rate of 0.08 mL/min. The calculation of molecular weights from the light-scattering detector was based on the known injected mass assuming 100% mass recovery. The content of thiazolidine-2-thione (TT) groups was determined spectrophotometrically on a Helios Alpha UV/vis spectrophotometer (Thermospectronic, UK) using the absorption coefficient for TT in methanol, $\epsilon_{305} = 10\,280\text{ L mol}^{-1}\text{ cm}^{-1}$. The amino acid analysis of the hydrolyzed samples (6 M HCl, 115 °C, 18 h in a sealed ampule) was performed on a Chromolith Performance RP-18e reversed-phase

column, 100 × 4.6 mm (Merck, Germany), using precolumn derivatization with phthalaldehyde and 3-sulfanylpropanoic acid (excitation at 229 nm, emission at 450 nm) and gradient elution with 10–100% of solvent B for 35 min at flow rate of 1.0 mL/min (solvent A: 0.05 M sodium acetate buffer, pH 6.5; solvent B: 300 mL of 0.17 M sodium acetate and 700 mL of methanol). MALDI TOF spectroscopy was carried out using a Bruker Biflex III mass spectrometer.

Synthesis of Peptides and Their Derivatives (1–6). The loading of the 2-chlorotriethyl chloride resin with Fmoc-amino acid in DCM in the presence of DIPEA (4 equiv) was assessed by the spectrophotometric determination of the Fmoc group (0.37 mmol/g) released with 25% piperidine in DMF. The linear fully protected heptapeptide was assembled using an AVSP-2 multiple automatic peptide synthesizer (Development Workshops of the Institute of Organic Chemistry and Biochemistry, Academy of Sciences of the Czech Republic), starting from the C-terminus using standard Fmoc procedures, by consecutive addition of the *N*-Fmoc-protected amino acid (2.5 equiv), PyBOP (2.5 equiv), HOBt (2.5 equiv), and DIPEA (5.0 equiv) in DMF. The Fmoc groups were removed using piperidine–DMF (1:4). The Fmoc-(Fmoc-Hmb)Ala-OH derivative was used for the incorporation of the Ala residue following Leu in peptides 3 and 4. The following Fmoc-Ala-OH (10 equiv) was coupled as its symmetric anhydride preformed with DIC (10 equiv) in 50% DMF–DCM. Fmoc-Glu(OtBu)-Ser($\psi^{Me,Me}$ pro)-OH and Fmoc-Lys-(Boc)-Ser($\psi^{Me,Me}$ pro)-OH pseudoproline dipeptides were used for the synthesis of peptides 5 and 6, respectively. Cleavage of the protected peptides from the resin was performed with a 30% solution of HFIP in DCM, 25 mL/g of resin, for 2 h. The resin was filtered off and rinsed with DCM, the filtrate was concentrated under vacuum, and the oily residue was precipitated with Et₂O. The precipitate was isolated by filtration and dried in vacuum. The yields were typically 90–99% based on the resin substitution with the first amino acid. Protected peptides 1–6 were characterized by MALDI-TOF MS (Table 1).

Table 1. Basic Characteristics of Protected Heptapeptides 1–6

compd ^a	structure	theor mol wt ^b	measd mol wt ^c
1	Fmoc-Val-Ala-Ala-Leu-Glu(OtBu)-Lys(Boc)-Glu(OtBu)-OH	1192.66	1215.64
2	Fmoc-Val-Ala-Ala-Leu-Lys(Boc)-Glu(OtBu)-Lys(Boc)-OH	1235.71	1258.68
3	Fmoc-Val-Ala-(AcHmb)Ala-Leu-Glu(OtBu)-Lys(Boc)-Glu(OtBu)-OH ^d	1370.73	1393.47
4	Fmoc-Val-Ala-(AcHmb)Ala-Leu-Lys(Boc)-Glu(OtBu)-Lys(Boc)-OH ^d	1413.73	1436.50
5	Fmoc-Val-Ala-Ala-Leu-Glu(OtBu)-Ser($\psi^{Me,Me}$ pro)-Glu(OtBu)-OH	1091.58	1114.21
6	Fmoc-Val-Ala-Ala-Leu-Lys(Boc)-Ser($\psi^{Me,Me}$ pro)-Lys(Boc)-OH	1177.66	1200.23

^aSample numbering used in the text. ^bCalculated monoisotopic molecular weight of the peptide acid. ^cM + Na relative molecular weight values from MALDI-TOF analysis. ^dAcHmb = 2-acetoxy-4-methoxybenzyl.

Reverse phase HPLC of the crude product showed a single peak (Chromolith C18 column, gradient 50–100% acetonitrile in water for 10 min, 0.1% TFA, 2 mL/min, UV detection at 220 nm), indicating that no further purification was necessary.

Fmoc Condensation (Peptides 7–18). TentaGel Rink amide resin (0.5 g, 0.1 mmol of Fmoc groups) was deprotected with 25% PIP in DMF and washed with DMF and DMSO. Fully protected heptapeptides 1–6 (0.05 mmol) were attached to the amino group of the resin in DMSO using DIC (0.1 mmol) as a coupling agent. The condensation was carried out for 6 h at 25 °C. The resin was incubated with acetic anhydride (10 equiv) and DIPEA (20 equiv) in DMF for 30 min to end-cap possible unreacted amino groups. The

peptide resin was washed with DMF, deprotected with 25% PIP and 2% DBU in DMF, and washed again with DMF and DMSO. The condensation (with 0.15 mmol of the protected heptapeptide), acetylation, deprotection, and washing steps were repeated until the desired number of heptad repeats (3 or 4) was assembled. Then the peptide resin was condensed with Fmoc-Peg₄ (2.5 equiv) using PyBOP (2.5 equiv), HOBt (2.5 equiv), and DIPEA (5.0 equiv) in DMF. After removal of Fmoc, the N-terminus was modified with Fmoc-Cys(Trt)-OH (the Fmoc group was removed, and the N-terminus was acetylated to obtain peptides 7–10) or 5-azidopentanoic acid (for peptides 11–16) under the same conditions as described above. The peptides were cleaved from the resin with a mixture of TFA–EDT–thioanisole–phenol–H₂O–TIPS (68.5:10:10:5.5:5:1) (peptides 7–10) or TFA–H₂O–TIPS (95:2.5:2.5) (peptides 11–16). For peptides 17 and 18, the N-terminal valine residue was modified with Fmoc-Peg₂₇ in two consecutive condensation and deprotection steps and acetylated. The crude peptides were purified on a semipreparative Chromolith C18 column using a gradient elution of acetonitrile–water with 0.1% TFA. For the basic characteristics of peptides 7–18, see Table 2. Examples of HPLC chromatograms and MALDI TOF MS spectra are shown in Figure S1.

Table 2. Basic Characteristics of Coiled Coil Peptides 7–18

compd ^a	structure ^b	theor mol wt ^c	measd mol wt ^d
7	Ac-Cys-Peg ₄ -(VAALEKE) ₃	2588.40	2589.54
8	Ac-Cys-Peg ₄ -(VAALKEK) ₃	2585.56	2586.98
9	Ac-Cys-Peg ₄ -(VAALEKE) ₄	3370.82	3371.69
10	Ac-Cys-Peg ₄ -(VAALKEK) ₄	3367.03	3368.79
11	5-azidopentanoyl-Peg ₄ -(VAALEKE) ₃	2610.45	2611.61
12	5-azidopentanoyl-Peg ₄ -(VAALKEK) ₃	2607.61	2608.69
13	5-azidopentanoyl-Peg ₄ -(VAALEKE) ₄	3350.85	3351.75
14	5-azidopentanoyl-Peg ₄ -(VAALKEK) ₄	3347.06	3347.72
15	5-azidopentanoyl-Peg ₄ -(VAALESE) ₄	3186.60	3185.81
16	5-azidopentanoyl-Peg ₄ -(VAALKSK) ₄	3179.02	3179.95
17	Ac-Peg ₂₇ -Peg ₂₇ -(VAALEKE) ₄	5628.21	5626.65
18	Ac-Peg ₂₇ -Peg ₂₇ -(VAALKEK) ₄	5624.42	5623.13

^aSample numbering used in the text. ^bSingle letter amino acid abbreviations of the peptide sequences are in parentheses. Ac = acetyl. ^cCalculated monoisotopic molecular weight of the peptide acid. ^dM + H relative molecular weight values from MALDI-TOF analysis.

Synthesis of Monomers. *N*-(2-Hydroxypropyl)methacrylamide (HPMA) was prepared by the reaction of methacryloyl chloride with 1-aminopropan-2-ol in DCM.¹⁵ *N*-Methacryloylglucylglycine (Ma-GG-OH) was prepared by the Schotten–Baumann acylation of glucylglycine with methacryloyl chloride in aqueous alkaline medium.¹⁶ 3-(*N*-Methacryloylglucylglycyl)thiazolidine-2-thione (Ma-GG-TT) was prepared by the reaction of Ma-GG-OH with 4,5-dihydrothiazole-2-thiol in DMF in the presence of *N,N'*-dicyclohexylcarbodiimide.¹⁷

Reactive Copolymer with TT Groups (19). The copolymer poly(HPMA-*co*-Ma-GG-TT) was prepared by radical solution copolymerization of HPMA (90 mol %) and Ma-GG-TT (10 mol %) performed in DMSO at 50 °C for 6 h. The concentration of monomers in the copolymerization mixture was 15% w/w, and that of AIBN initiator was 2% w/w.¹⁷ The molecular weight parameters of polymer 19 are $M_w = 24\,000$ and $M_w/M_n = 1.5$.

Copolymer with Propargyl Groups and Biotin (20). *N*-(2-Aminoethyl)biotinamide hydrobromide (1.1 mg, 3.0 μmol), polymer 19 (50 mg, 39 μmol of TT groups), and DIPEA (1 μL, 5.8 μmol) were dissolved in DMF (0.8 mL). Propargylamine (26 μL, 0.39 mmol) was

added 15 min later. After 15 min, the polymer was precipitated with diethyl ether and isolated by centrifugation. The crude product was dried, dissolved in water, purified on Sephadex G-25 (PD 10 column), and lyophilized to yield 44 mg of white polymer 20. The biotin content was 1.8% w/w, as determined by HABA assay.¹⁸ The molecular weight parameters of polymer 20 are $M_w = 28\,000$ and $M_w/M_n = 1.6$.

Attachment of Coiled Coil Peptides to the Polymer Precursor via “Click” Reaction: Example of Preparation (21, 22). Copolymer 20 (5 mg, 3 μmol of propargyl groups), peptide azide 13 (4 mg, 1.2 μmol), and sodium ascorbate (1.6 mg, 8 μmol) were dissolved in 0.2 mL of water, and the solution was thoroughly bubbled with Ar to remove oxygen. A 0.8 M oxygen-free solution of copper(II) sulfate (4 μL, 3.2 μmol) was added. The progress of the reaction was monitored by HPLC; all peptide azide was bound to the polymer within 30 min. The polymer–peptide conjugate was separated by SEC on Sephadex G-25 column in water and lyophilized to yield 7 mg of polymer–peptide conjugate 21. The content of the peptide in the copolymer as determined by amino acid analysis was 40% w/w. Polymer–peptide conjugate 22 was prepared analogously starting with peptide azide 14. The molecular weight parameters of polymer 21 are $M_w = 56\,000$, $M_w/M_n = 1.7$ and of polymer 22 are $M_w = 55\,000$, $M_w/M_n = 1.7$.

Preparation of the Polymer–scFv Complex via Coiled Coil Interactions. Polymer 21 was dissolved in PBS buffer (0.7 mg/mL) and mixed with a solution of the fusion protein–scFv-K (0.7 mg/mL) in volume ratios of 1:1, 1:4, and 1:8 (corresponding to molar ratios 8:1, 2:1, and 1:1 between the peptide E and the peptide K). The resulting complex was characterized by SEC, gel electrophoresis, and analytical ultracentrifugation.

CD Spectroscopy. CD measurements were performed using Jasco-815 dichrograph. The spectra were measured in 1 mm quartz cell from 190 to 260 nm with a scanning speed of 20 nm/min, a response time of 4 s, and two computer-averaged accumulations. The peptide concentration was kept constant at 0.2 mg/mL in sodium phosphate buffer. Temperature-dependent measurements were performed using a PTC-423S/L Peltier type temperature control system in a 1 cm quartz cell allowing for stirring of the measured solution (peptide concentration 0.02 mg/mL). The measurement was performed at 222 nm to indicate the α -helical content (temperature interval 2–95 °C, temperature gradient of 25 °C/h, response time of 32 s). The spectra were expressed as mean molar ellipticity at 222 nm per residue and were converted into α -helical fraction (f_H) using a two-state model.¹⁹

Analytical Ultracentrifugation. Sedimentation analysis was performed using a ProteomeLabXL-I analytical ultracentrifuge equipped with an An50Ti rotor (BeckmanCoulter). Compounds 17 and 18 were dissolved to a concentration of 0.4 mg/mL in 50 mM sodium phosphate (pH 7.4) and 150 mM NaCl buffer, which was also used as a reference, and the complex was prepared by mixing equal volumes of the individual solutions. A sedimentation velocity experiment was carried out at 48 000 rpm and 20 °C; absorbance scans were recorded at 230 nm in 20 min intervals with 30 μm spatial resolution. The buffer density and peptide partial specific volumes were estimated in SEDNTERP 1.09. The partial specific volume of Peg was estimated as 0.83 mL/g at 20 °C, and the partial specific volumes of compounds 17 and 18 were then calculated on the basis of the molar ratio of their peptide and Peg components. The data were analyzed with SEDFIT 12.1.²⁰ The scFv-K protein and polymer 21 were dissolved to a concentration of 0.7 mg/mL in 20 mM MES (pH 6.7) and 300 mM NaCl buffer, which was also used as a reference. For sedimentation analysis, equal volumes of protein and polymer solutions or protein and buffer solutions were mixed. The sedimentation velocity experiment was carried out at 45 000 rpm and 20 °C; absorbance scans were recorded at 280 or 240 nm in 5 min intervals with a spatial resolution of 30 μm. The sedimentation equilibrium experiment was performed at 4–6–8–10–12–14 000 rpm at 4 °C. Absorbance data were collected at 280 nm by averaging 20 scans with a spatial resolution of 10 μm after 30 h (first scan) or 18 h (consecutive scans) of achieving equilibrium and were globally

analyzed with SEDPHAT 8.2 using a noninteracting discrete species model.²¹ The buffer density, scFv-K partial specific volume, and dimensions of the sedimenting species were estimated in SEDNTERP. The partial specific volume of polymer **21** was estimated as 0.80 mL/g at 20 °C, and the average of the two values was used for the protein–polymer complex. The sedimentation velocity experiment with the scFv-K protein and the (VAALKEK)₄ peptide was conducted in the same way as for the free scFv-K protein, with the exception of the addition of 1:5 molar excess of the peptide. Some continuous size distributions were recalculated in SEDPHAT for better accuracy; these are given directly in *s*_{20,w} values corrected for temperature and solvent contributions and are thus shifted to higher values compared to the observed *s** calculated in SEDFIT.

Construction of the Expression Vector for the Protein with Fusion Sequence. Cloning of the scFv fragment derived from the monoclonal antibody M75, scFv M75, has already been described.¹² To introduce peptide K, i.e., (VAALKEK)₄, at the C-terminus of the scFv fragment, the 90 bp oligonucleotide duplex was synthesized as four complementary oligonucleotides (K1 = 5'-gtactgtggcagcgtgaa-gagaagggttgcggccttgaaa; K2 = 5'-gagaagggtggcggcactgaa-gaaaagggtcggcctctgaaagagaagg; K3 = 5'tgccgccaccttctcttcaaggccg-caaccttctcttcagcgtgccaca; K4 = 5'gtaccttctcttcagagcggcgaccttcttcag), where the 5' ends of K2 and K3 are phosphorylated (with T4 polynucleotide kinase) and the 5' ends of K1 and K4 contain four-base overhangs allowing cloning into the Acc65I site contained in the scFv M75 sequence between the myc-tag and C-terminal his-tag. Oligonucleotides K1 + K3 and K2 + K4 were annealed, the resulting duplexes were ligated, and a 90 bp oligoduplex was gel purified and cloned into the Acc65I-opened vector containing the sequence of scFv M75. Thus, the final construct codes for scFv M75 in the format V_H-*(gly₄ser)₄*-V_L-myc-Kpeptide-His₅.

Expression and Purification of the Fusion Protein scFv-K.

For expression in *E. coli* BL21(DE3) cells, a modified pET-22(b) vector was used in which the scFv coding sequence is preceded by the PelB signal sequence, allowing for translocation of the product into the periplasmic space, and followed by a His5 tag, allowing for product isolation and purification by IMAC chromatography on Ni-CAM (Sigma). Final purification was achieved by ion exchange chromatography on a MonoS column.

Receptor Binding ELISA. The binding activity of the polymer **21**–scFv complex formed via coiled coil interactions was assayed in the ELISA. The microtiter plates were coated overnight with the CA IX antigen (100 ng per well in 100 μL of bicarbonate buffer pH 9.6), blocked with 1% BSA in PBS, and treated with polymer **21**–scFv complexes prepared in molar ratios of 1:1, 1:4, and 1:8, respectively, for three different protein concentrations: 10, 2, and 0.4 mg/L. ScFv-K alone and unconjugated polymer **21** were used as the positive and negative controls, respectively. The bound polymer and polymer–scFv complex were detected with the streptavidin peroxidase (Px) conjugate, whereas for the positive control, scFv-K, which lacks biotin, the anti-pentaHis monoclonal antibody conjugated with peroxidase was used. The color developed in the reaction catalyzed by peroxidase was measured at 492 nm.

RESULTS AND DISCUSSION

Design and Synthesis of the Peptides. The repeating heptapeptide sequences were chosen according to the general rules described^{22–24} for the formation of coiled coil heterodimers. Briefly, the coiled coil motif contains two to six α-helices forming a left-handed superhelical bundle. The essential feature of the peptides forming the coiled coil motif is a repeated heptapeptide sequence denoted *a-b-c-d-e-f-g*. A helical wheel diagram (Figure 1) was used to design the peptide sequences forming the intermolecular heterodimers used in this work. The positions *a* and *d* are occupied with hydrophobic residues, whereas the *e* and *g* positions are usually occupied with charged or hydrophilic residues. The choice of the hydrophobic amino acid residues at positions *a* and *d*

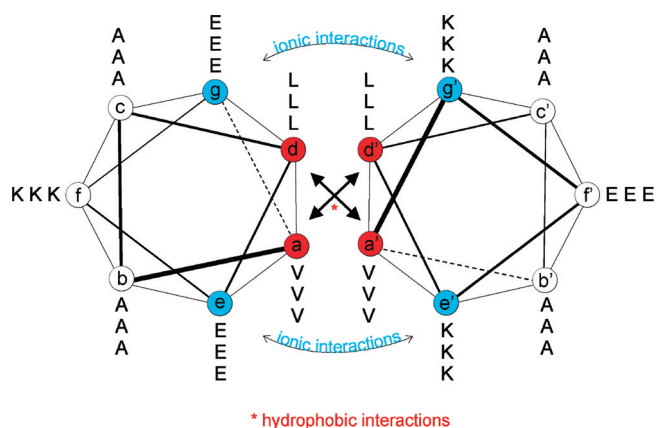


Figure 1. Helical wheel diagram depicting the peptide sequences (VAALEKE)₃ and (VAALKEK)₃ designed to form an antiparallel coiled coil heterodimer.

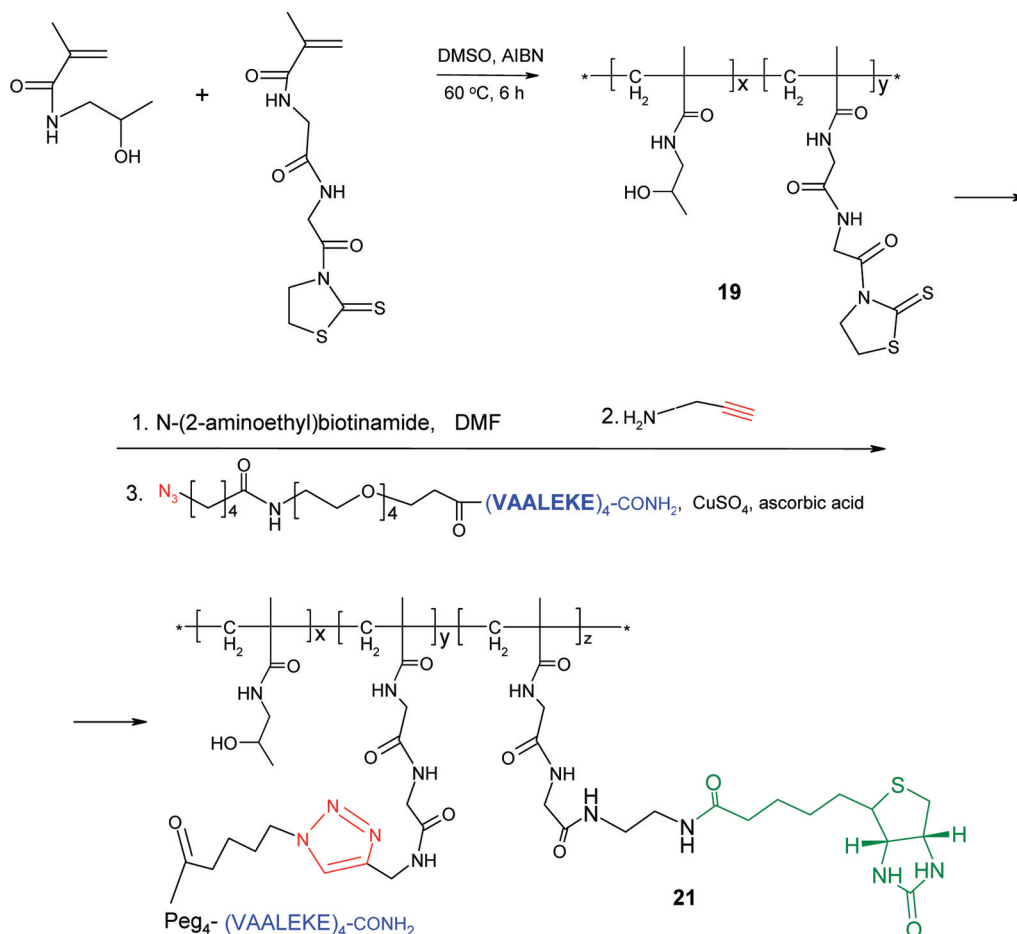
determines the association number of the helices in the superhelix. Placement of valine and leucine at the *a* and *d* positions, respectively, promotes the formation of dimeric coiled coils. The ionic interactions between residues in the *e* and *g* positions of the two helices substantially contribute to the stability of the coiled coil and, depending on the charge of the side chain, may control the formation of either homo- or heterodimers. Therefore, glutamic acid was placed at positions *e* and *g* of one strand, and lysine occupied the *e'* and *g'* positions of the other strand. The electrostatic attraction between the oppositely charged residues drives the formation of the heterodimeric coiled coil. Eventual homodimerization is thermodynamically less favorable due to the electrostatic repulsions between the like charges of the same sequence. Positions *b* and *c* were filled with alanine, which is known for its high α-helical propensity. Lysine and glutamic acid were placed in the remaining *f* and *f'* positions to balance the total charge of the peptides and increase their solubility. We have also tried serine in positions *f* and *f'*. Serine is hydrophilic and neutral in terms of its helical propensity. However, the main reason for the use of serine was the possibility of using so-called pseudoproline dipeptides during the solid phase peptide synthesis. These consist of a dipeptide in which a Ser (or Thr) residue is protected as a proline-like oxazolidine. Incorporation of these derivatives into the structure of a protected peptide dramatically improves its solubility and, as a result, improves the yield of the subsequent condensation reactions.

Although Figure 1 shows the two peptides in an antiparallel orientation, we are aware of the possibility to obtain eventually a parallel arrangement. We believe that in the final complex formed between polymer **21** and the recombinant protein scFv-K the antiparallel orientation would be enforced by spatial requirements.

Protected heptapeptides **1–6** were prepared by standard solid phase peptide synthesis using the Fmoc/*t*-Bu strategy on a 2-chlorotrityl chloride resin. Solid phase fragment condensation of protected heptapeptides **1** and **2** (followed by N-terminal modification) afforded peptides **7–14** with three or four heptad repeats in relatively low yields (between 10 and 15% after HPLC purification).

2-Hydroxy-4-methoxybenzyl (Hmb) derivatives of amino acids have been reported²⁵ to substantially improve yields and the solubility of peptide sequences that are difficult to obtain.

Scheme 1



The use of Hmb-protected heptapeptides 3 and 4 led to a slightly increased yield (15–20%) of fragment condensation; however, the benefit was paid off by more laborious and expensive preparation of derivatives 3 and 4 compared with protected heptapeptides 1 and 2.

Much more significant improvement in the efficiency of the synthesis was achieved using oxazolidine derivatives 5 and 6. Thus, peptides 15 and 16, containing the VAALESE and VAALKSK sequences, respectively, were prepared by solid phase fragment condensation in higher yield and purity (30–40% after HPLC purification). Unfortunately, the stability of the corresponding coiled coil heterodimers, determined by a measurement of the temperature dependence of the ellipticity at 222 nm, was lower compared with the peptides based on the original VAALEKE and VAALKEK repeating motifs.

Polymer–Peptide Conjugates. Initially, we intended to attach the coiled coil peptides to the polymers using addition of the cysteine thiol group of peptides 7–10 to pendant maleimidyl groups incorporated in the polymer. Unfortunately, we have encountered several difficulties with this approach. First, it was quite difficult to remove all traces of thiol scavengers from the crude peptide detached from the resin after the solid phase synthesis, even with preparative HPLC.

These impurities also react with the maleimidyl groups, thus significantly lowering the yield of the polymer–peptide conjugate. Second, the maleimidyl groups also react, albeit slowly, with the primary amino groups of the lysine residues. This results in unwanted branching of the final product as we

confirmed by SEC (Figure S2). Therefore, we turned our attention to another chemoselective conjugation technique, alkyne–azide cycloaddition.

Synthesis of the polymer–peptide conjugates 21 and 22 was based on the copper-catalyzed “click” reaction of peptide azides 13 and 14 with polymer precursor 20 containing propargyl groups (Scheme 1). The alkyne–azide cycloaddition was a very efficient and chemoselective method of binding unprotected peptides to polymer carriers.

The HPMA-based copolymers described above contain multiple peptides attached to the polymer backbone via a short tetra(ethylene glycol) spacer. The polymer precursors 19 and 20 have a polydispersity of about 1.5, which is typical for polymers prepared by classical radical polymerization. After attachment of the multiple peptide sequences to the side chain of the polymers, the resulting conjugates become even more heterogeneous in terms of the number of peptides per one polymer chain. Although this should not be a major problem regarding the biological activity of the final product, its exact physicochemical characterization is much more difficult.

Hence, we also prepared better defined poly(ethylene glycol) derivatives of the coiled coil peptides as an alternative to the polymer–peptide conjugates based on HPMA copolymers. Attachment of two Peg₂₇ molecules to the coiled coil peptides with four heptad repeats resulted in well-defined monodisperse block copolymers 17 and 18 with molecular weights of 5628 and 5624, respectively (MALDI-TOF MS). The association

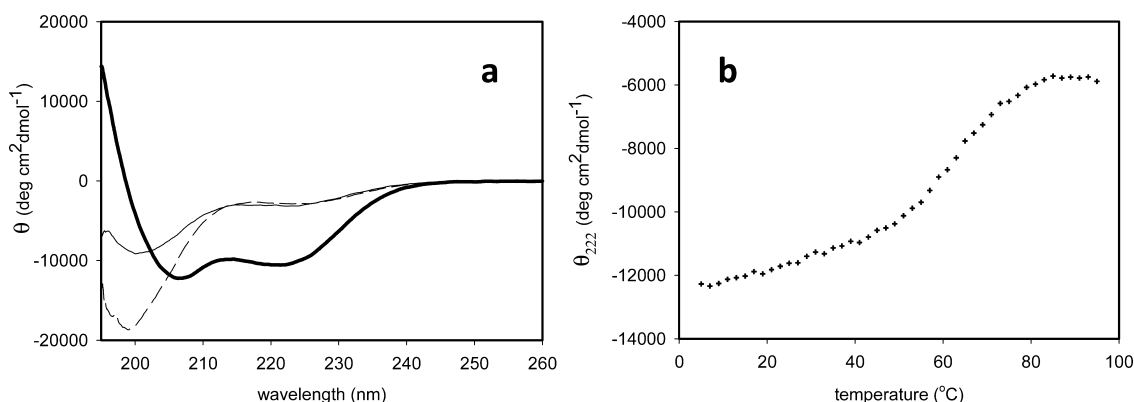


Figure 2. CD spectra of the peptides 7 and 8 and their equimolar mixture (a) (solid line, 8; dashed line, 7; solid thick line, 7 + 8) and thermal melting profiles in an equimolar mixture (b).

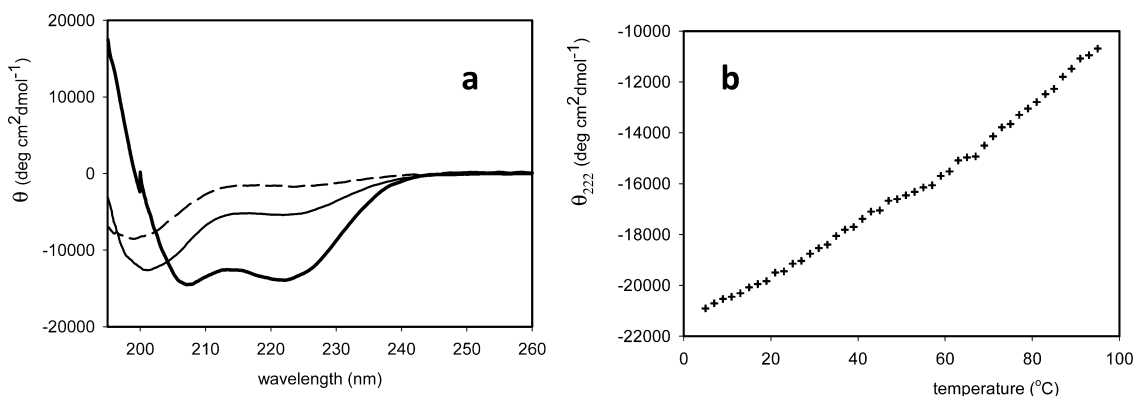


Figure 3. CD spectra of peptides 9 and 10 and their equimolar mixture (a) (solid line, 10; dashed line, 9; solid thick line, 9 + 10) and thermal melting profiles in an equimolar mixture (b).

behavior of the two copolymers was studied using analytical ultracentrifugation and CD spectroscopy.

Circular Dichroism. Although two-dimensional NMR spectroscopy has been recently used⁹ for detailed characterization of heterodimeric coiled coils, CD spectroscopy is still the most important analytical tool for study of similar systems. It has been used also in this work for the determination of the secondary structure of the peptides, their mixtures, and polymer–peptide conjugates. As peptides 7–18 show CD spectra typical for an unfolded structure, we can assume that formation of the α -helix upon addition of the other complementary peptide is most likely caused by formation of a coiled coil heterodimer consisting of the two complementary peptides.

First, peptides 7 and 8 containing three heptapeptide repeats were prepared. Their N-termini were modified with tetra-(ethylene glycol) spacer and *N*-acetylcysteine, enabling attachment to polymers with maleimidyl groups. Although CD spectra of these peptides alone did not show significant content of helical structure, their equimolar mixture exhibited minima at 208 and 222 nm, which are typical for α -helix. Nevertheless, the intensity of these minima is lower than could be expected for typical α -helical conformation (Figure 2a).

Similar results were obtained with analogous peptides 9 and 10 consisting of four repeated heptads. In this case, the proportions of α -helical fractions in the peptides 9 and 10 were 22% and 13%, respectively. Their mixture exhibited a significantly higher α -helical content than the preceding sample ($f_H = 43\%$). The ratio of the mean residual ellipticity at 222 and

208 nm was very close to 1, which is typical for a coiled coil arrangement (Figure 3a).

Attempts to use cysteinyl peptides 7–10 for conjugation to the polymers were unsuccessful; therefore, we switched to azide-terminated peptides 11–16. Peptides 11–12 containing only three heptad repeats exhibited typical CD spectra for a random coil conformation. Surprisingly, no significant changes in the CD spectra were observed even after mixing their equimolar amounts (Figure S3).

Analogous peptides 7 and 8, containing *N*-acetylcysteine instead of 5-azidopentanoic acid as the terminal residue, have shown a typical α -helix pattern. A possible explanation of this phenomenon is the dimerization of the cysteinyl peptides via disulfide bridges. We have observed spontaneous formation of the disulfide in PBS buffer due to air oxidation using HPLC analysis. The peak corresponding to the disulfide gradually rose over time; however, it completely disappeared after the addition of a large excess of the reducing agent tris(2-carboxyethyl)-phosphine (TCEP). Unfortunately, we were not able to obtain reliable CD spectra in the presence of TCEP; at the relevant concentration of TCEP, the total UV absorption of the solution below 220 nm was too high. We speculate that formation of the disulfide contributes to the higher thermodynamic stability of the coiled coil heterodimer.

To increase the stability of the coiled coil heterodimers that were eventually formed, peptides 13–18 containing four heptad repeats were investigated. While the individual peptides showed typical random coil like CD, upon mixing with the complementary peptide, the CD spectra displayed α -helix

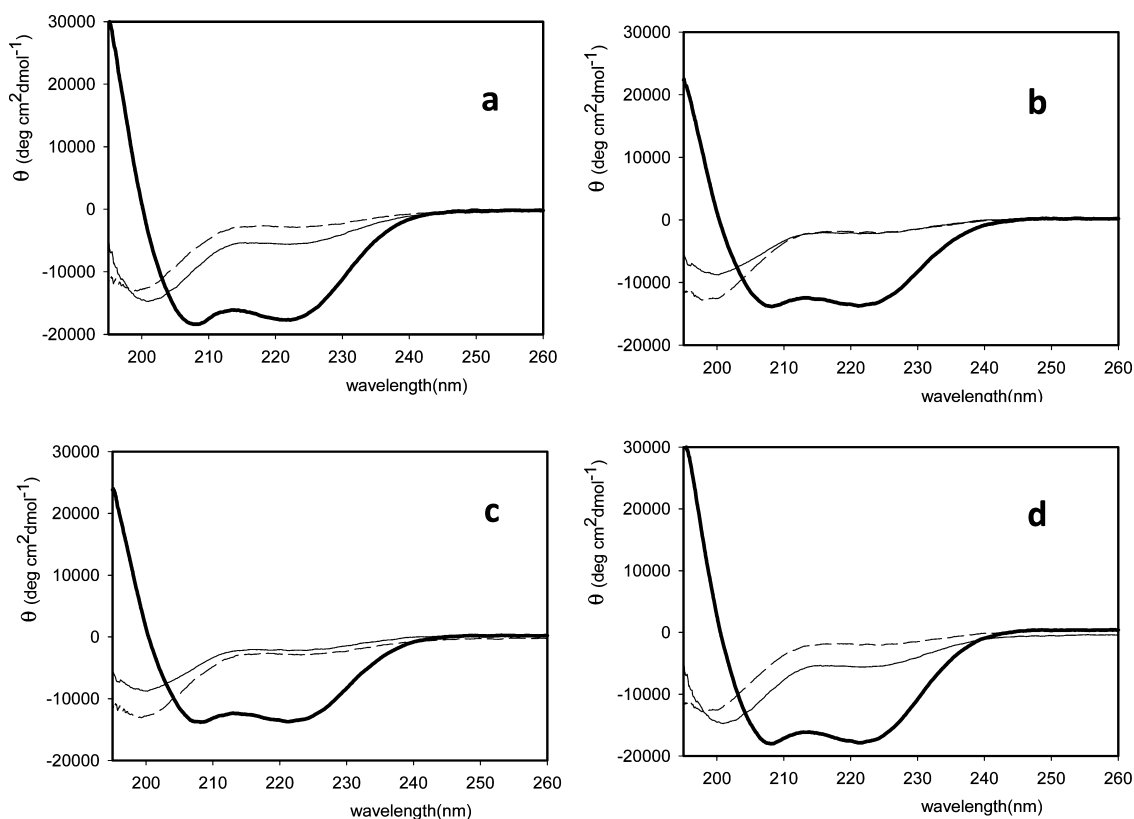


Figure 4. CD spectra of the peptides and their equimolar mixtures: (a) solid line, 14; dashed line, 13; solid thick line, 13 + 14; (b) solid line, 16; dashed line, 15; solid thick line, 15 + 16; (c) solid line, 16; dashed line, 13; solid thick line, 13 + 16; (d) solid line, 14; dashed line, 15; solid thick line, 15 + 14.

pattern. This has been observed for the following pairs of peptides: 13 + 14, 15 + 16, 17 + 18, 13 + 16, and 14 + 15 (Figure 4).

Peptides 17 and 18 contain a monodisperse poly(ethylene glycol) chain consisting of 54 oxyethylene units. Their association behavior was investigated using both CD spectroscopy and analytical ultracentrifugation. The CD spectrum of the equimolar mixture of the two peptides (Figure 6a) had a typical α -helix shape. Moreover, the calculated¹⁸ α -helical fraction in the mixture was 100%, which was significantly higher than that in the mixtures of the other pairs of coiled coil peptides. This finding is in accordance with the previously reported^{10,11} helix-stabilizing effect of Peg.

After proper characterization of the association behavior of the coiled coil peptides 13–18, we decided to verify our initial idea to use the coiled coil interaction for the noncovalent connection of two large macromolecules using the polymer–peptide conjugates 21 and 22. Upon mixing equimolar amounts of the two polymers in PBS buffer, we observed a significant increase in the molecular weight compared to the original polymers (from 45 000 to 385 000), as measured by SEC with a LS detector. At the same time, changes in the CD spectra were evident, suggesting a high content of α -helical structure. Surprisingly, polymer–peptide conjugate 22 alone has shown a substantial degree of helicity; however, this was increased further after the addition of polymer–peptide conjugate 21 (Figure 7a).

Melting Curves. The thermal stability of the coiled coil heterodimers was verified by measuring the temperature dependence of the ellipticity at 222 nm. Loss of the secondary helical structure in the peptide mixture upon heating is

manifested by an increase in the Θ_{222} value. The inflex point of the curve corresponds to the melting temperature of the α -helix.

The coiled coil heterodimer prepared from peptides 7 and 8 consisting of three heptapeptide repeats exhibited a typical melting curve with a melting temperature of 60 °C (Figure 2b). An analogous mixture of peptides 9 and 10 (containing four heptads) showed much higher thermal stability with a melting point of 90 °C (Figure 3b). This finding can be explained by the cooperative behavior of the coiled coil interaction.

Heterodimers based on azide-terminated peptides 11–16 revealed less stable but distinct helices for the mixture of the longer peptides 13 and 14 (melting temperature of 61 °C, Figure 5); no significant portion of α -helix for the shorter peptides 11 and 12 was found. The thermal helix stability of 13 and 14 is almost the same as that of the mixture of shorter peptides 7 and 8; however, it is much lower than that of the analogous cysteinyl peptides 9 and 10. We attribute this fact to the stabilization of the latter peptides by disulfide bridges spontaneously formed in aqueous solutions by air oxidation.

A mixture of peptides 15 and 16 containing serine in the heptapeptide repeating unit melted at 51 °C (Figure 5), indicating a somewhat lower stability of the coiled coil heterodimer compared to the coiled coil prepared from peptides 13 and 14. The coiled coil heterodimers made of “cross-mixed” peptides 13 + 16 and 14 + 15 had melting temperatures of 55 and 53 °C, respectively (Figure 5). As a result, we decided to use only the more stable VAALKEK/VAALKEK repeating motif in subsequent preparations of the peptide–polymer conjugates.

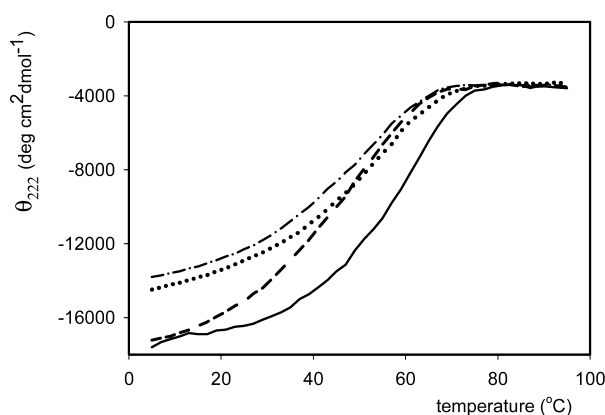


Figure 5. Thermal melting profiles of equimolar mixtures of peptides **13** and **14** (solid line); **15** and **16** (dashed-dotted line); **13** and **16** (dotted line); and **14** and **15** (dashed line).

It has been mentioned that peptides **17** and **18** containing poly(ethylene glycol) (Peg) with 54 repeating ethylene glycol units were prepared to investigate the effect of the monodisperse polymer on the associative behavior of the coiled coil peptides. We have also studied the influence of the short Peg chain on the thermal stability of the coiled coil. Although it has been reported^{10,11} that attachment of Peg to the coiled coil peptide increases the melting temperature of the α -helix, we did not observe any significant difference in the thermal stability of the coiled coil heterodimers when comparing the “Pegylated” peptides **17** and **18** (melting at 57 °C, Figure 6b) with the “non-Pegylated” peptides **13** and **14** (melting at 61 °C, Figure 5). Although the presence of the Peg chain did not increase the melting temperature of the coiled coil peptides, the content of the α -helical fraction of the “Pegylated” coiled coil heterodimer was significantly higher compared to the “non-Pegylated” heterodimer.

In contrast, a mixture of the HPMA-based polymer–peptide conjugates **21** and **22** exhibited higher thermal stability than peptides without a polymer. Unfortunately, it is very difficult to determine the exact melting temperature of the sample, as the melting curve does not show any significant inflex point. It is a practically linear dependence with a relatively mild slope compared to the steep melting curves of peptides **13**–**18**. This finding is in accordance with previously reported work¹⁹ describing the stabilization effect of the HPMA copolymer on the coiled coil formation. The effect is likely caused by cooperative interactions of multiple coiled coil peptides grafted to the polymer chain.

Analytical Ultracentrifugation. Sedimentation analysis of compounds **17** and **18** and their complex was hampered by the fact that both molecules are relatively small and do not contain a chromophore moiety. Therefore, the time for sedimentation analysis had to be prolonged substantially, and measuring at a short wavelength was necessary. Both facts negatively affected the resolution of the analysis. Nevertheless, the sedimentation velocity experiment proved complex formation in a rather convincing way (Figure 8). The sedimentation coefficients $s_{20,w}$ determined for compounds **17** and **18** were 0.57 and 0.52 ± 0.1 S, respectively, whereas their mixture exhibited a single peak of 0.84 ± 0.08 S in the sedimentation coefficient distribution. Sedimentation coefficient values correspond to a molecular weight of approximately 6 ± 1 kDa for both compounds **17** and **18** or 11 ± 2 kDa for

their mixture, indicating quantitative complex formation. However, while the sedimentation equilibrium data proved that the mixture of compounds **17** and **18** behaves like a heavier particle than its components, all equilibrium data displayed shifts resembling aggregation and were therefore not evaluated (data not shown).

Noncovalent Polymer–scFv Antibody Fragment Conjugate Formed by Coiled Coil Interaction. For the ultimate proof of the feasibility of the concept of noncovalent conjugation of a targeting antibody fragment to the polymer carrier via coiled coil interaction, we chose a recombinant single-chain fragment of the monoclonal antibody M75 (directed against human carbonic anhydrase IX) engineered to contain the (VAALKEK)₄ peptide near its C-terminus and capable of forming a coiled coil heterodimer with the partner peptide (VAALEKE)₄ present in the structure of the HPMA copolymer.

The construction and expression of the scFv M75 fragment carrying peptide (VAALKEK)₄ at its C-terminus (scFv-K) are described in detail in the Materials and Methods section. Briefly, into the already existing scFv M75 DNA, an oligonucleotide duplex coding for (VAALKEK)₄ was introduced between the myc epitope and C-terminal his-tag, and the final construct in the pET-22(b) vector was expressed in *E. coli* BL21(DE3) cells. Following two chromatography steps, the purified scFv-K protein (32 158 Da) was characterized using SDS-PAGE, gel filtration, and analytical ultracentrifugation.

The recombinant product is highly pure and homogeneous, as shown by SDS-PAGE (Figure 9a, lane 2); however, the SEC (Figure 9b) and analytical ultracentrifugation (Figure S4) indicate the formation of a homodimer. The sedimentation coefficient of the scFv-K protein was determined by a sedimentation velocity experiment as $s_{20,w} = 3.57 \pm 0.1$ S (Figure S4a). This value is higher than s_{max} , the theoretical maximum sedimentation coefficient for a spherical particle of a given scFv-K monomer mass, indicating scFv-K oligomerization. The easiest explanation of these data would be an elongated dimer with approximate dimensions of 15×3 nm for a cylinder-shaped molecule. Indeed, the sedimentation equilibrium experiment (Figure S4b), enabling direct calculation of the mass of sedimenting species, resulted in a z-average molecular mass of $61\,399 \pm 453$ Da for a non-interacting discrete species model, indicating formation of the scFv-K dimer. As the recombinant scFv without the (VAALKEK)₄ fusion sequence behaves as a monomer in solution (Figure 9b), it is possible to conclude that the scFv-K dimerization is promoted by the presence of the (VAALKEK)₄ peptide in the fusion protein, possibly through its unexpected homotypic interaction. This interpretation is also in agreement with the finding that polymer–peptide conjugate **22** alone showed a substantial degree of helicity. The addition of an excess of free peptide (VAALEKE)₄ leads to the disruption of the protein homodimer and the formation of the heterodimer peptide–protein, as shown in the AUC experiment in Figure S5. Surprisingly, we have found larger particles in the mixture with a sedimentation coefficient of 4.00 S that might correspond to a heterotrimeric complex consisting of two protein molecules and one or more peptides.

The addition of scFv-K to polymer **21** (containing peptide E) resulted in a product with a molecular weight significantly exceeding that of both components, as shown by analytical ultracentrifugation analysis (Figure S6). The data from the sedimentation equilibrium experiment (Figure S6b) could not

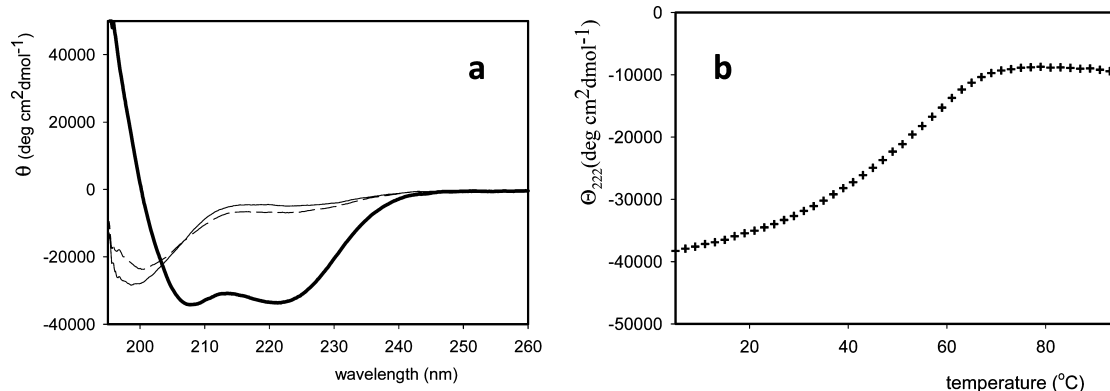


Figure 6. CD spectra of peptides **17** and **18** and their equimolar mixture (a) (solid line, **18**; dashed line, **17**; solid thick line, **17 + 18**) and thermal melting profiles in an equimolar mixture (b).

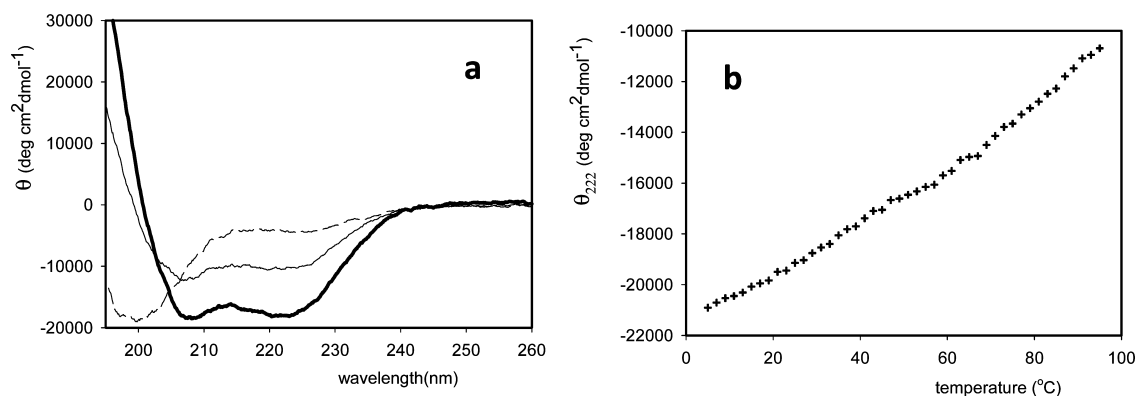


Figure 7. CD spectra of copolymers **21** and **22** and their equimolar mixture (solid line, **22**; dashed line, **21**; solid thick line, **21 + 22**) (a) and thermal melting profiles in an equimolar mixture (b).

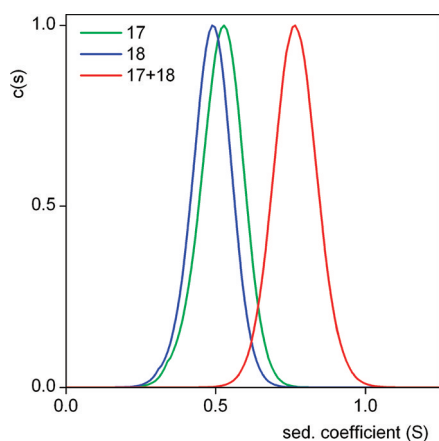


Figure 8. Sedimentation analysis of compounds **17** and **18** and their noncovalent complex. Individual compounds and their equimolar mixture were analyzed in an analytical ultracentrifuge as described in the Materials and Methods section. The plot shows the normalized superposition of the resulting distributions of the sedimentation coefficients of the species sedimenting in the analyzed samples as calculated with the Sedfit program.

be fitted with either a single or two species model. However, the addition of a third independent particle into the calculation resulted in good fit with approximate *z*-average molecular weights in the ranges of 60–90, 120–150, and 200–500 kDa. These numbers do not correspond to the true masses of the sedimenting species, but they reflect the complexity or the

heterogeneity of the analyzed sample. This observation is in perfect agreement with the results of the sedimentation velocity experiment (Figure S6a), showing the formation of at least three distinct particles with sedimentation coefficients of 4, 6, and 8 S, with a smaller fraction of even larger conjugates (8–16 S). As shown in Figure 10, it is unlikely that the 4 S complex particles could correspond to unbound scFv-K protein because the 0.5 S difference between the sedimentation coefficients of free scFv-K protein and 4 S particles of the scFv-K–polymer **21** complex is too large to be ascribed to calculation error. As polymer **21** seems to be completely associated in complex formation (Figure 10, the absence of polymer **21** peak at 2 S), it is more likely that the scFv-K dimer dissociated completely due to coiled coil heterodimer formation with polymer **21**. The different particles observed in the complex mixture represent different polymer **21**–scFv-K stoichiometries, with the dominant one being the 1:1 complex corresponding to the 4 S particle and higher stoichiometries (more scFv-K molecules bound to one polymer **21** molecule) corresponding to larger particles.

Receptor Binding of the Polymer–Protein Complex.

The ELISA experiment (Figure 11) has shown that the scFv M75–polymer complex binds efficiently to its cognate antigen CA IX. This proves that the coiled coil interaction between peptide sequences comprising four repeats of VAALKEK on the part of the antibody fragment and VAALEKE on the part of polymer can serve as a universal noncovalent and non-destructive attachment of the targeting protein to the polymeric carrier.

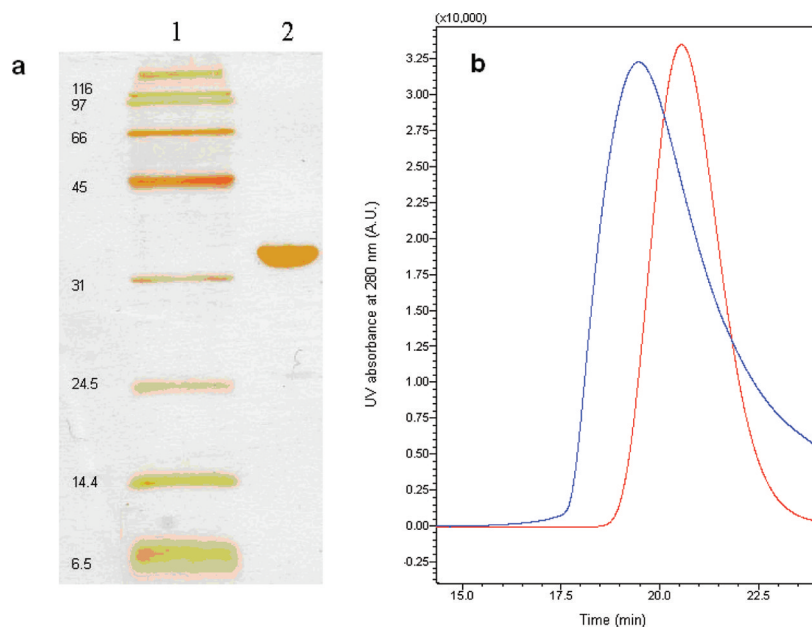


Figure 9. Characterization of the recombinant scFv-K protein by SDS-PAGE (a) and SEC (b). SDS-PAGE was performed on a 15% polyacrylamide gel. Lane 1: standards of molecular weights in kDa (BioRad); lane 2: purified scFv-K. SEC was performed on a Superose 12 PC 3.2/30 column (Pharmacia) in 0.05 M phosphate buffer with 0.15 M NaCl, pH 6.5, at a flow rate of 0.08 mL/min. Blue line: scFv-K; red line: scFv without the fusion peptide K.

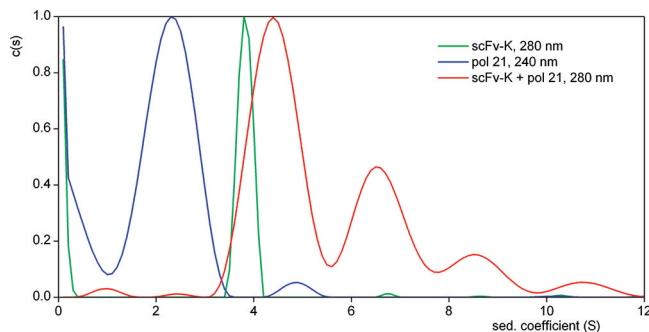


Figure 10. Comparison of normalized size distributions of individual complex components as well as the complex analyzed at two different wavelengths calculated with the Sedphat program as detailed in the Materials and Methods section.

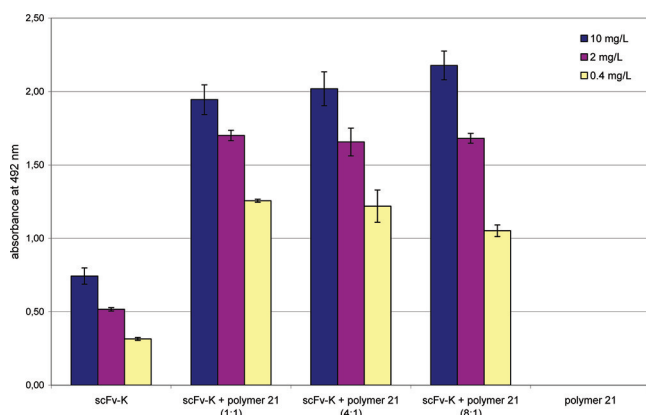


Figure 11. CA IX antigen binding by the protein-polymer complex evaluated by ELISA at three different concentrations. From left to right: scFv-K alone (positive control, detection by anti-pentaHis-Px); scFv-K + polymer 21 (1:1, 4:1, 8:1 w/w), and polymer 21 (negative control, detection by streptavidin-Px).

The presence of the K-peptide at the C-terminal of the engineered scFv-K does not interfere with its ability to bind to the CA IX antigen, nor does it interfere with his-tag recognition by the anti-pentaHis antibody in the ELISA (Figure 11, scFv-K bars). Figure 11 gives only a qualitative result of receptor binding. It is impossible to quantitatively compare the binding efficiency of the scFv-K protein alone and the polymer-protein complex due to different methods of evaluation. While the polymer-protein complex was detected using a biotin label on the polymer, the scFv-K protein was detected with an anti-pentaHis antibody.

Nevertheless, the ELISA has clearly shown that the polymer-protein complex binds to the antigen due to the specific interaction between the scFv-K ligand and CA IX. The polymer alone (without the targeting ligand) was used as a negative control and has shown no binding.

The multivalency of the polymer 21 allows binding of up to eight scFv-K molecules per one polymer chain. The formation of the complexes containing more than one scFv-K was confirmed by sedimentation analysis (Figure 10). Surprisingly, we have found no significant differences between the levels of binding of polymer-protein complexes containing different amounts of scFv-K. We hypothesize that this observation can be explained by steric hindrance when more than one scFv-K ligand is attached to one polymer chain. If one scFv-K is already bound to the receptor, the other ligands cannot effectively interact with another CA IX molecule.

We plan to prepare more homogeneous complexes using semitelechelic polymers synthesized by controlled radical polymerization techniques (e.g., RAFT, ATRP). More detailed biological evaluation of the polymer-protein complexes will be a subject of the upcoming publications.

CONCLUSIONS

A new water-soluble polymer carrier system for potential targeted drug delivery has been designed, prepared, and

characterized. A biotinylated HPMA-based copolymer containing pendant peptide sequences (VAALEKE)₄ has been synthesized. Recombinant protein consisting of the scFv fragment of the M75 antibody and the fusion peptide sequence (VAALKEK)₄ was expressed and isolated from *E. coli*. The protein formed a stable complex with the copolymer due to formation of coiled coil heterodimers between the complementary peptides. The polymer–protein complex exhibited specific binding to the immobilized antigen in the ELISA. We believe that the presented HPMA copolymer–coiled coil system can be used as a universal tool for the attachment of recombinant targeting proteins to synthetic polymers, thus providing a receptor-specific drug carrier suitable for neoplastic treatment or diagnosis.

■ ASSOCIATED CONTENT

● Supporting Information

Examples of SEC and HPLC chromatograms, MALDI TOF MS spectra and CD spectra of peptides, sedimentation analysis data with residual plots. This material is available free of charge via the Internet at <http://pubs.acs.org>.

■ AUTHOR INFORMATION

Corresponding Author

*E-mail: pechar@imc.cas.cz.

■ ACKNOWLEDGMENTS

The work was supported by the Grant Agency of the Czech Republic, grant 203/08/0543, and by the Ministry of Education of the Czech Republic, grant IM4635608802, and in part by project AV0Z50520514 awarded by the Academy of Sciences of the Czech Republic. We especially acknowledge Anna Vaňková for excellent technical assistance in peptide synthesis.

■ REFERENCES

- (1) Kopeček, J. *Eur. J. Pharm. Sci.* **2003**, *20*, 1–16.
- (2) Maeda, H.; Matsumura, Y. *Crit. Rev. Ther. Drug Carrier Syst.* **1989**, *6*, 193–210.
- (3) Etrych, T.; Strohalm, J.; Kovář, L.; Kabešová, M.; Říhová, B.; Ulbrich, K. *J. Controlled Release* **2009**, *140*, 18–26.
- (4) Kovář, M.; Mrkvan, T.; Strohalm, J.; Etrych, T.; Ulbrich, K.; Štastný, M.; Říhová, B. *J. Controlled Release* **2003**, *92*, 315–330.
- (5) Hongrapipat, J.; Kopečková, P.; Liu, J.; Prakongpan, S.; Kopeček, J. *Mol. Pharmaceutics* **2008**, *5*, 696–709.
- (6) Wu, K. S.; Liu, J. H.; Johnson, R. N.; Yang, J. Y.; Kopeček, J. *Angew. Chem., Int. Ed.* **2010**, *49*, 1451–1455.
- (7) Apostolovic, B.; Deacon, S. P. E.; Duncan, R.; Klok, H.-A. *Macromol. Rapid Commun.* **2011**, *32*, 11–18.
- (8) Apostolovic, B.; Klok, H.-A. *Biomacromolecules* **2010**, *11*, 1891–1895.
- (9) Deacon, S. P. E.; Apostolovic, B.; Carbajo, R. J.; Schott, A. K.; Beck, K.; Vicent, M. J.; Pineda-Luceda, A.; Klok, H.-A.; Duncan, R. *Biomacromolecules* **2011**, *12*, 19–27.
- (10) Pechar, M.; Kopečková, P.; Joss, L.; Kopeček, J. *Macromol. Biosci.* **2002**, *2*, 199–206.
- (11) Vandermeulen, G. W. M.; Tziatzios, C.; Klok, H.-A. *Macromolecules* **2003**, *36*, 4107–4114.
- (12) Závada, J.; Zavadová, Z.; Pastorek, J.; Biesová, Z.; Ježek, J.; Velek, J. *Br. J. Cancer* **2000**, *82*, 1808–1813.
- (13) Král, V.; Mader, P.; Collard, R.; Fabry, M.; Hořejší, M.; Řezáčová, P.; Kožíšek, M.; Závada, J.; Sedláček, J.; Rulisek, L.; Brynda, J. *Proteins* **2008**, *71*, 1275–1287.
- (14) Li, Y.; Wang, H.; Oosterwijk, E.; Selman, Y.; Mira, J. C.; Medrano, T.; Shiverick, K. T.; Frost, S. C. *Biochem. Biophys. Res. Commun.* **2009**, *386*, 488–492.
- (15) Ulbrich, K.; Šubr, V.; Strohalm, J.; Plocová, D.; Jelínková, M.; Říhová, B. *J. Controlled Release* **2000**, *64*, 63–79.
- (16) Rejmanová, P.; Labský, J.; Kopeček, J. *Makromol. Chem.* **1977**, *178*, 2159–2168.
- (17) Šubr, V.; Ulbrich, K. *React. Funct. Polym.* **2006**, *66*, 1525–1538.
- (18) Green, N. M. *Biochem. J.* **1965**, *94*, C23.
- (19) Rohl, C. A.; Baldwin, R. L. *Methods Enzymol.* **1998**, *295*, 1–26.
- (20) Schuck, P. *Biophys. J.* **2000**, *78*, 1606–1619.
- (21) Schuck, P. *Anal. Biochem.* **2003**, *320*, 104–124.
- (22) Mason, J. M.; Arndt, K. M. *ChemBioChem* **2004**, *5*, 170–176.
- (23) Apostolovic, B.; Danial, M.; Klok, H.-A. *Chem. Soc. Rev.* **2010**, *39*, 3541–3575.
- (24) Yu, Y. B. *Adv. Drug Delivery Rev.* **2002**, *54*, 1113–1129.
- (25) Quibell, M.; Turnell, W. G.; Johnson, T. *J. Chem. Soc., Perkin Trans. 1* **1995**, 2019–2024.
- (26) Yang, J. Y.; Xu, C. Y.; Wang, C.; Kopeček, J. *Biomacromolecules* **2006**, *7*, 1187–1195.